Antibody conjugated magnetic PLGA nanoparticles for diagnosis and treatment of breast cancer

Jaemoon Yang,[a] Choong-Hwan Lee,[b] Joseph Park,[a] Sungbaek Seo,[a] Eun-Kyung Lim,[a] Yong Jin Song,[c] Jin-Suck Suh,[d] Ho-Geun Yoon,[e] Yong-Min Huh*[d] and Seungjoo Haam*[a]

Received 28th February 2007, Accepted 17th April 2007
First published as an Advance Article on the web 27th April 2007
DOI: 10.1039/b702538f

DOX–magnetic PLGA nanoparticles conjugated with well-tailored antibodies were synthesized for the detection and therapy of breast cancer. Magnetic nanocrystals embedded in polymeric nanoparticles did not inhibit the nanoparticle formulation or drug release kinetics. The multimodal nanoparticles demonstrated remarkable cancer cell affinity and ultrasensitivity *via* magnetic resonance imaging. Furthermore, the loaded anticancer drugs were released and sustained for three weeks.

1. Introduction

Inorganic/organic nanoparticles hold significant potential for biomedical applications due to their molecular size.[1] Recently, highly crystalline and monodisperse magnetic nanocrystals (MNCs) have demonstrated excellent properties that can be applied to areas such as drug delivery, magnetic resonance (MR) imaging, cell separation and hyperthermia.[2–5] In general, MNCs are combined with organic compounds such as small ligands or biocompatible polymers, for various applications.[6] For example, organic ligands on the MNC surface were exchanged with hydrophilic, functionalized ligands to mediate conjugation with a peptide or antibody.[3] Furthermore, the MNCs were used as seeds to polymerize the monomers.[7] Unfortunately, these approaches demand sophisticated procedures or preparatory stages for preparation of organo-magnetic hybrids.

In the present study, we synthesized a multimodal nanocomposite using inorganic/organic materials for detection and treatment of cancer (see Scheme 1). The nano-emulsion method was used to incorporate the anticancer drug doxorubicin (DOX) into magnetic poly(D,L-lactide-*co*-glycolide) (PLGA) nanoparticles (DMPNP). The physico-chemical properties of the nanoparticles were evaluated for nanostructure and characteristic features. The antibody Herceptin® (HER) used for targeting breast cancer was conjugated to DMPNP using bioconjugation chemistry (HER-DMPNP). The breast cancer cell binding affinity of HER-DMPNP and its potential as an MR probe were estimated. To assess the therapeutic potential of HER-DMPNP, the drug loading content, entrapment efficiency and release behavior were also investigated.

[a]*Department of Chemical Engineering, Yonsei University, Seoul 120-749, South Korea. E-mail: haam@yonsei.ac.kr; Fax: +82-2-312-6401; Tel: +82-2-2123-3554*
[b]*ATGen, Advanced Technology Research Center, 68 Yatap-dong, Bundang-gu, Seongnam-si, Gyeonggi-do, 463-816, South Korea*
[c]*Department of Physics, College of Natural Science, Ajou University, Suwon 433-749, South Korea*
[d]*Department of Radiology, College of Medicine, Yonsei University, Seoul 120-752, South Korea*
[e]*Department of Biochemistry and Molecular Biology, Center for Chronic Metabolic Disease Research, College of Medicine, Yonsei University, Seoul 120-752, South Korea*

2. Experimental

2.1. Materials

Polyoly(D,L-lactide-*co*-glycolide) (PLGA, M_w: 5 000) was obtained from Wako Chemicals. Iron(III) acetylacetonate, 1,2-hexadecanediol, dodecanoic acid, dodecylamine, benzyl ether, 1-ethyl-3-(3-dimethylaminopropyl)carbodiimide, *N*-hydroxy-succinimide and polyvinyl alcohol (PVA, M_w: 15 000–20 000) were purchased from Sigma-Aldrich. Doxorubicin (DOX) was obtained from Fluka. Phosphate buffered saline (PBS; 10 mM, pH 7.4) was purchased from Gibco. All other chemicals and reagents were of analytical grade.

2.2. Synthesis of magnetic nanocrystals (MNCs)

For the synthesis of the MNCs, 2 mmol iron(III) acetylacetonate, 10 mmol 1,2-hexadecanediol, 6 mmol dodecanoic acid, 6 mmol dodecylamine, and benzyl ether (20 mL) were mixed

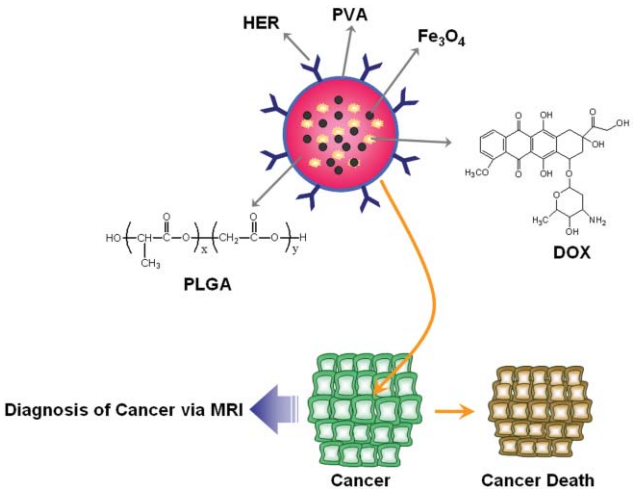

Scheme 1 Schematic illustration of magnetic PLGA nanoparticles for diagnosis and treatment of cancer.

under a nitrogen atmosphere. The mixture was preheated to 150 °C for 30 min and refluxed at 300 °C for 30 min. After the reactants were cooled to room temperature, the products were purified with an excess of pure ethanol. Approximately 12 nm of MNCs were synthesized after the seed-mediated growth.[3,8]

2.3. Preparation of DOX–magnetic PLGA nanoparticles (DMPNP)

PLGA (100 mg), MNCs (20 mg), DOX (5 mg) and triethylamine (50 μL) were dissolved in 10 mL of dichloromethane. The organic phase was added to 20 mL of an aqueous phase containing 3% PVA as a stabilizer. After mutual saturation of the organic and aqueous phases, the mixture was emulsified for 10 min with an ultrasonicator (ULH700S, Ulssohitech) operated at 450 W.[9] After solvent evaporation, the products were purified with three cycles of centrifugation at 20 000 rpm. The precipitated nanoparticles were redispersed in 10 mM sodium phosphate buffer (2 mL, pH 7.4). Due to the presence of amphiphilic PVA, the prepared nanoparticles were well suspended in the aqueous phase. The PLGA nanoparticles (PNPs) and DOX-PLGA nanoparticles (DPNPs) were prepared in the same manner as previously mentioned.

2.4. Characterization of DOX–magnetic PLGA nanoparticles (DMPNP)

The size distribution of the nanoparticles was analyzed by laser scattering (ELS-Z, Otsuka electronics). The morphology and presence of MNCs were evaluated using a transmission electron microscope (TEM, JEM-1100, JEOL Toko). DPNP and DMPNP were negatively stained with phosphotungstic acid.[10] Fourier transform infrared spectroscopy (FT-IR, ExcaliburTM series, Varian Inc.) was used to confirm the characteristic bands of the DMPNP. The saturation magnetizations of the MNC and DMPNP were evaluated using a vibrating-sample magnetometer (VSM, MODEL-7300, Lakeshore). The quantity of MNCs encapsulated in the DMPNP was analyzed with a thermogravimetric analyzer (SDT-Q600, TA instrument). The surface compositions were evaluated by X-ray photoelectron spectroscopy (XPS, ESCALAB MK II, V.G. Scientific Ltd.).

2.5. Drug release test

The drug loading content, entrapment efficiency and drug release profile were determined using a UV spectrophotometer (Optizen 2120UV, MECASYS Co). To obtain the drug release profiles, 20 mg of DPNP and DMPNP were suspended in 5 mL of PBS sealed in dialysis tubing and immersed in 20 mL of buffer solution at 37.5 °C. The system was shaken at a moderate speed and the amount of DOX released was monitored at λ_{max} (480 nm) over regular time intervals. In addition, the drug loading content and entrapment efficiency were also measured in the same manner.

2.6. Antibody conjugation with DMPNP (HER-DMPNP)

In order to conjugate the antibody with the prepared DMPNP, 1 mg of HER (Herceptin®, Roche Pharma Ltd.) was dissolved in 400 μL of PBS and mixed with 100 μL of the DMPNP solution (10 mg mL^{-1}). *N*-Hydroxysuccinimide (2.0 mM) and 1-ethyl-3-(3-dimethylaminopropyl)carbodiimide (2.0 mM) were added to the previous solution. After 4 h, HER-DMPNP were purified with a Sephacryl S-300 column (Amersham Biosciences). A BCA kit was used to measure the amount of HER conjugated to the DMPNP surface.[3]

2.7. Cell affinity test

The cancer cell affinity of HER-DMPNP was investigated using flow cytometry and epifluorescence microscopy. Target cancer cells (NIH3T6.7, SK-BR3 and MDA-MB-231 cells, 10^6 cells mL^{-1}) were incubated and treated with HER-DMPNP for 30 min. The solution was washed three times with 0.2% fetal bovine serum (FBS) and 0.02% NaN_3 in PBS. The samples were resuspended in 400 μL 4% paraformaldehyde and FACScalibur (Beckton-Dickinson, Mansfield, MA) was used to monitor the cell-associated fluorescence. The DOX was excited with an argon laser (488 nm) and fluorescence was detected at 560 nm. Data were collected and analyzed from 10 000 gated events.

2.8. *In vitro* MR imaging procedure

All MR imaging experiments were performed with a 1.5 T clinical MRI instrument with a micro-47 surface coil (Intera; Philips Medical Systems, Best). For T2-weighted MR imaging of *in vitro* cells at 1.5 T, the following parameters were adopted: point resolution: 156 × 156 μm, section thickness of 0.6 mm, TE = 60 ms, TR = 4000 ms and number of acquisitions = 1. For T2 mapping of *in vitro* cells, the following parameters were adopted: point resolution of 156 × 156 μm, section thickness of 0.6 mm, TE = 20, 40, 60, 80, 100, 120, 140, 160 ms, TR = 4000 ms and number of acquisitions = 2. R2 was defined as 1/T2 s^{-1}.

3. Results and disscusion

MNCs were synthesized using the high temperature seed-mediated growth method for magnetic components of MR probes for cancer detection. The MNC morphology was examined by TEM, as shown in Fig. 1(a). The MNC size was determined by laser scattering to be 12.6 ± 0.5 nm.

DMPNP for MR probes and drug carriers were prepared by the nano-emulsion method in the presence of DOX, MNC and PLGA. Similarly, PNP was formulated without DOX or MNC for reference. TEM images of PNPs and DMPNPs are presented in Fig. 1(b) and (c). MNCs dispersed in organic PVA solvent were well encapsulated in the polymeric nanoparticles due to the hydrophobic interaction of MNCs and PLGA. Using laser scattering, the sizes of PNP and DMPNP were 68.5 ± 7.2 nm and 76.8 ± 6.2 nm, respectively. Compared to PNP, the DMPNP size slightly increased due to incorporation of MNC.

The solubility of MNC and DMPNP is shown in Fig. 2. The oil phase of hexane exists above water due to its lower density. The MNC was soluble only in hexane and the DMPNP was dispersed only in water due to the surface PVA. The nonionic surfactant, PVA, successfully increased the water solubility of DMPNP. Furthermore, after several days, the DMPNP was

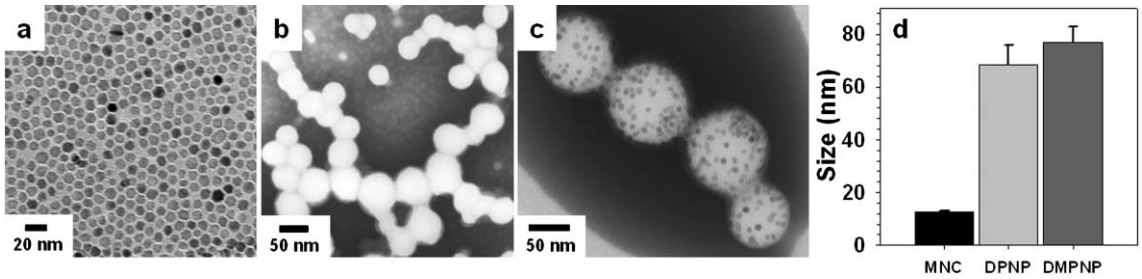

Fig. 1 TEM images of (a) MNC in hexane, (b) DOX-PLGA nanoparticles (DPNP), (c) DMPNP in an aqueous solution and (d) laser scattering size distributions of MNC, DPNP and DMPNP.

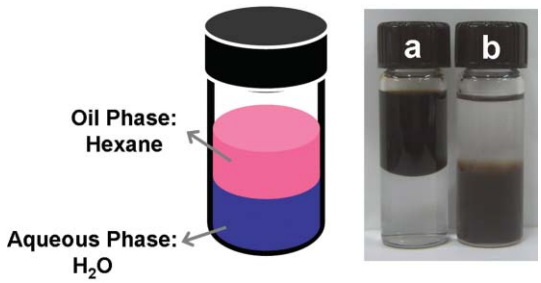

Fig. 2 Solubility test of (a) MNC in hexane and (b) DMPNP in an aqueous phase.

well dispersed in the aqueous phase. To this end, DMPNP demonstrated excellent colloidal stability in an aqueous phase (Fig. 2).

For the assessment of the potential of DMPNP as an MR probe, the magnetic sensitivity was estimated. The hysteresis loops of MNC and DMPNP were investigated using a vibrating sample magnetometer at 300 K (Fig. 3(a)). The MNC and DMPNP exhibited superparamagnetic behavior without magnetic hysteresis. The saturation magnetizations at 0.9 T of MNC and DMPNP were 74.7 emu g^{-1} and 32.5 emu g^{-1}, respectively. Due to the presence of organic components such as DOX, PLGA and PVA, the saturation magnetization of DMPNP was lower than that of MNC. The quantity of magnetic nanoparticles in DMPNP was measured using a thermogravimetric analyzer and the results are shown in Fig. 3(b). All organic compounds were removed at

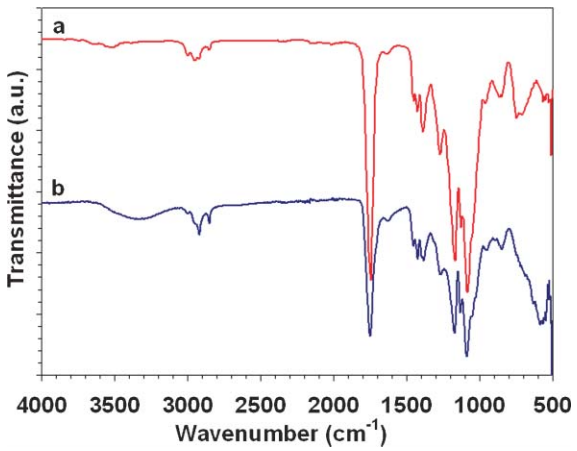

Fig. 4 FT-IR spectra of (a) PLGA and (b) DMPNP.

210–270 °C. The quantity of MNC encapsulated in DMPNP was 23.1 wt%.

FT-IR was used to evaluate the chemical structure of PLGA (Fig. 4(a)) and DMPNP (Fig. 4(b)). The characteristic peak of PLGA at 1749 cm^{-1} is due to the ester group (Fig. 4(a)). During preparation of DMPNP, the characteristic peak of PLGA was not altered (Fig. 4(b)). The hydroxy group of PVA was confirmed at 3500–3100 cm^{-1} (Fig. 4(b)). Furthermore, the MNC characteristic peak of the Fe–O bond was observed at 585 cm^{-1}.[11] These results suggest that the MNC of DMPNP successfully coexisted with PLGA due to the presence of PVA.

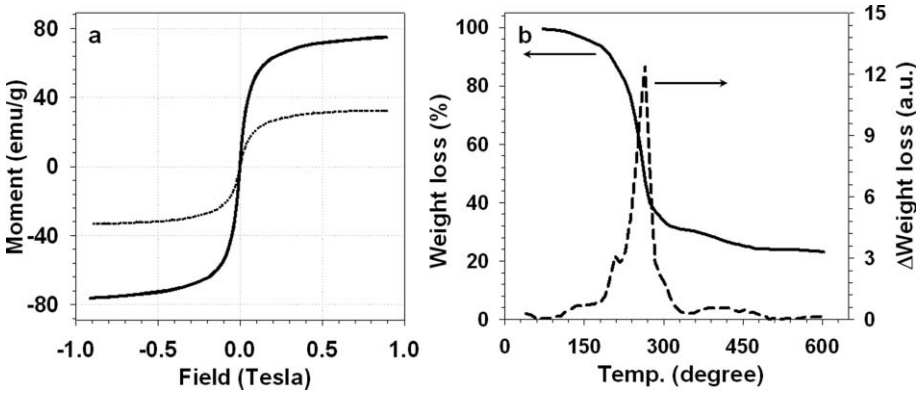

Fig. 3 (a) Magnetic hysteresis loops of MNC (black solid line) and DMPNP (dotted line). (b) Thermogravimetry analysis of DMPNP: weight loss *vs.* temperature (black solid line), Δ weight loss *vs.* temperature (dashed line).

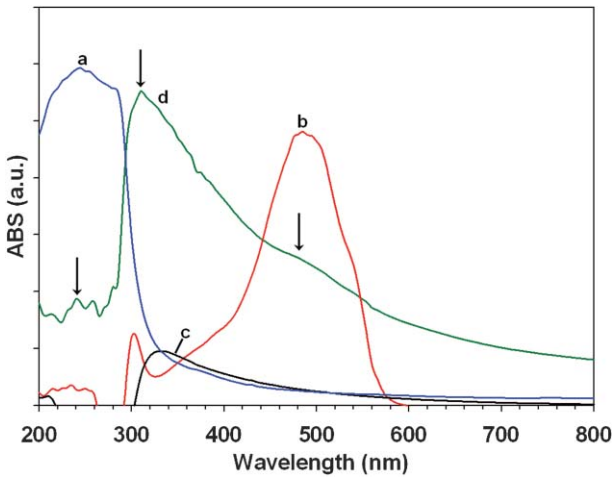

Fig. 5 UV-vis adsorption spectra of (a) MNC in hexane, (b) DOX, (c) PNP and (d) DMPNP in an aqueous solution.

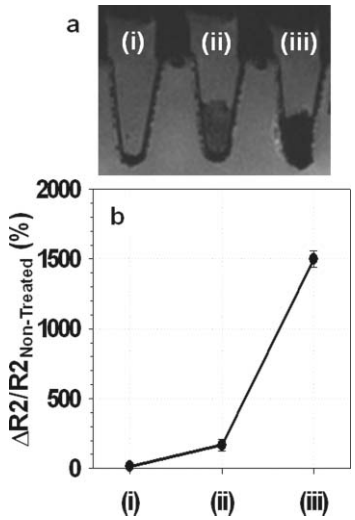

Fig. 7 (a) T2-weighted MR images and (b) $\Delta R2/R2_{Non\text{-}treated}$ graph for (i) MDA-MB-231, (ii) SK-BR3 and (iii) NIH3T6.7 cells.

To further confirm the DMPNP multi-structure, UV-vis absorption spectroscopy was performed (Fig. 5). The characteristic bands of MNC, DOX and PLGA were observed at 245 nm, 485 nm and 335 nm, respectively. The characteristic bands of DMPNP are shown in Fig. 5(d).

The breast cancer cell targeting efficacy of HER-DMPNP was investigated. The human epidermal growth factor receptor-2 (HER2) was used as a tumor targeting marker for the treatment of patients with metastatic breast cancer.[12] Fibroblast NIH3T6.7 cells, which express high levels of the HER2/neu cancer markers, were compared with SK-BR3 and MDA-MB-231 cells, which express low levels of the cancer markers.[3] In Fig. 6(a), the NIH3T6.7 cells incubated with HER-DMPNP demonstrated a greater fluorescence intensity by FACS analysis than other cells, and the relative intensity was 87.4 times higher than that of non-treated cells. Compared to non-treated control cells, the relative fluorescence intensities of SK-BR3 and MDA-MB-231 cells were 6.5 and 1.5, respectively. In addition, the cellular binding efficiency of HER-DMPNP to the NIH3T6.7 cells was visualized using an epifluorescence microscope (Fig. 6(c)). The red is due to DOX of the HER-DMPNPs in the target cells (the blue of the nucleus is due to 4′,6-diamidino-2-phenylindole (DAPI) staining), indicating acceptable cellular binding efficiency. FACS analysis and fluorescence microscopy demonstrated that HER-MFND successfully bound target cancer cells.

The T2-weighted MR images and the change of relaxivity figure for three types of breast cancer cell lines indicated the potential for cancer detection (Fig. 7). The MR image of NIH3T6.7 cells incubated with HER-DMPNP exhibited a black color. Other cells presented gray due to low levels of the cancer markers. The changes of $\Delta R2/R2_{Non\text{-}treated}$ in the HER-DMPNP treated cells compared to the non-treated cells were ~1 500% (NIH3T6.7), ~166.7% (SK-BR3) and ~14.3% (MDA-MB-231), as shown in Fig. 7(b). These results demonstrated the efficient targeted delivery of HER-DMPNP for the HER2/neu receptor of cancer cells.

To test the influence of MNCs in polymeric nanoparticles on the drug release profile, a release test was performed in triplicate to calculate a mean value and standard deviation. The quantities of encapsulated DOX in DPNP and DMPNP were 17.4% and 5.8%, respectively. However, the drug entrapment efficiencies for DPNP and DMPNP were 62.7%

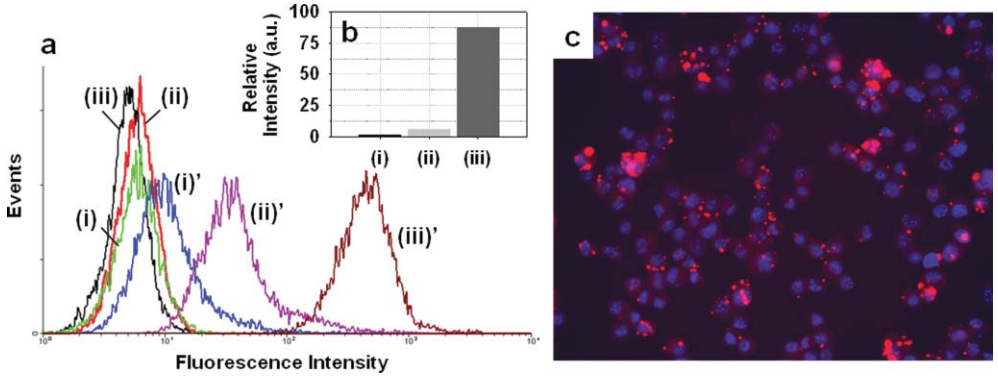

Fig. 6 (a) FACS analysis of HER-DMPNP against (i)′ MDA-MB-231, (ii)′ SK-BR3 and (iii)′ NIH3T6.7 cells. The non-treated control cells are also presented: (i) MDA-MB-231, (ii) SK-BR3 and (iii) NIH3T6.7 cells. (b) Relative intensity *via* FACS analysis. (c) Fluorescence microscopy image of NIH3T6.7 cells incubated with HER-DMPNP; red: DOX and blue: DAPI.

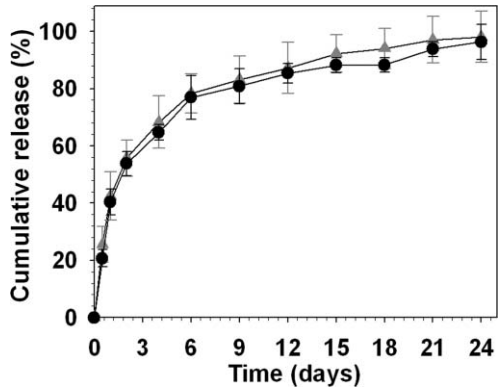

Fig. 8 The drug release profiles for (▲) DPNP and (●) DMPNP.

and 67.9%, respectively. The amount of encapsulated drug in DMPNP was lower than that in DPNP due to the presence of the MNC. The drug entrapment efficiencies were analogous for both cases. Similarly, the drug release profiles of DPNP and DMPNP were comparable (Fig. 8). After 3 and 12 days, 60% and 80% of the encapsulated DOX was released from DPNP and DMPNP due to polymer degradation. To this end, DOX loaded DMPNP was released from drug carriers without any inhibition due to MNC.

Conclusions

We successfully synthesized antibody conjugated DOX–magnetic PLGA nanoparticles (HER-DMPNP) for detection and treatment of cancer. The well-tailored DMPNP was prepared using a surfactant through a nano-emulsion method. MNC was embedded in polymeric nanoparticles through hydrophobic interaction. The DMPNP demonstrated excellent sensitivity as MR probes for detection of cancer cells. Moreover, affinity of the HER-DMPNP to cancer cells was predominant. In addition, DOX encapsulated in polymeric nanoparticles released sustainably without any inhibition due to the presence of MNC. These multifunctional nanocomposites can be applied to various biomedical fields such as targeted drug delivery, MRI probes and cell separation.

Acknowledgements

This work was supported by KOSEF through National Core Research Center for Nanomedical Technology (R15-2004-024-00000-0 and R01-2006-000-10023-0), the National R&D Program for Cancer Control, Ministry of Health & Welfare, Republic of Korea (0620190-1), and Yonsei University Research Fund of 2006.

References

1 P. Alivisatos, *Science*, 1996, **271**, 933; W. Li, C. Gao, H. Qian, J. Ren and D. Yan, *J. Mater. Chem.*, 2006, **16**, 1852; Y.-W. Jun, Y.-M. Huh, J.-S. Choi, J.-H. Lee, H.-T. Song, S.-J. Kim, S. Yoon, K.-S. Kim, J.-S. Shin, J.-S. Suh and J. Cheon, *J. Am. Chem. Soc.*, 2005, **127**, 5732; Y. Li, M. Afzaal and P. O'Brien, *J. Mater. Chem.*, 2006, **16**, 2175.
2 S. Rana, A. Gallo, R. S. Srivastava and R. D. K. Misra, *Acta Biomater.*, 2007, **16**, 233.
3 Y.-M. Huh, Y. Jun, H. Song, S. Kim, J. Choi, J. Lee, S. Yoon, K. Kim, J. Shin, J. Suh and J. Cheon, *J. Am. Chem. Soc.*, 2005, **127**, 12387; J. Lee, Y.-M. Huh, Y. Jun, J. Seo, J. Jang, H. Song, S. Kim, E. Cho, H. Yoon, J. Suh and J. Cheon, *Nat. Med.*, 2006, **13**, 95.
4 T. Schneider, L. R. Moore, Y. Jing, S. Haam, P. S. Williams, A. J. Fleischman, S. Roy, J. J. Chalmers and M. Zborowski, *J. Biochem. Biophys. Methods*, 2006, **68**, 1.
5 S. I. Park, Y. H. Hwang, J. H. Lim, J. H. Kim, H. I. Yun and C. O. Kim, *J. Magn. Magn. Mater.*, 2006, **304**, 403.
6 X. Michalet, F. F. Pinaud, L. A. Bentolila, J. M. Tsay, S. Doose, J. J. Li, G. Sundaresan, A. M. Wu, S. S. Gambhir and S. Weiss, *Science*, 2005, **307**, 538.
7 Y. Sun, X. Ding, Z. Zheng, X. Cheng, X. Hua and Y. Peng, *Chem. Commun.*, 2006, 2765.
8 S. Sun, H. Zeng, D. B. Robinson, S. Raoux, P. M. Rice, S. X. Wang and G. Li, *J. Am. Chem. Soc.*, 2004, **126**, 273.
9 J. Yang, S. B. Park, H. G. Yoon, Y.-M. Huh and S. Haam, *Int. J. Pharm.*, 2006, **324**, 185.
10 S. Sengupta, D. Eavarone, I. Capila, G. Zhao, N. Watson, T. Kiziltepe and R. Sasisekharan, *Nature*, 2005, **28**, 568.
11 C. Rocchiccioli-Deltcheff, R. Franck, V. Cabuil and R. Massart, *J. Chem. Res.*, 1987, **5**, 126.
12 R. M. Hudziak, G. D. Lewis, M. Winget, B. M. Fendly, H. M. Shepard and A. Ullrich, *Mol. Cell. Biol.*, 1989, **9**, 1165.